

# High-energy angle-resolved photoemission spectroscopy probing bulk correlated electronic states in quasi-one-dimensional $V_6O_{13}$ and $SrCuO_2$

S. Suga, A. Shigemoto, A. Sekiyama, S. Imada, A. Yamasaki, A. Irizawa, and S. Kasai  
*Graduate School of Engineering Science, Osaka University, Toyonaka, Osaka 560-8531, Japan*

Y. Saitoh

*Department of Synchrotron Research, Kansai Research Establishment, JAERI, SPring-8, Mikazuki, Hyogo 679-5148, Japan*

T. Muro

*JASRI, Mikazuki, Sayo, Hyogo 679-5198, Japan*

N. Tomita and K. Nasu

*Institute of Materials Structure Science, KEK, 1-1 Oho, Tsukuba 305-0801, Japan*

H. Eisaki

*National Institute of Advanced Industrial Science and Technology (AIST), Umezono, Tsukuba 305-8568, Japan*

Y. Ueda

*Institute for Solid State Physics, University of Tokyo, Kashiwanoha, Kashiwa 277-8581, Japan*

(Received 20 January 2004; published 20 October 2004)

Soft x-ray excited angle-resolved photoemission spectroscopy (ARPES) is performed for the valence bands of quasi-one-dimensional  $V_6O_{13}$  and  $SrCuO_2$  in order to reveal behavior of the strongly correlated V  $3d$  and Cu  $3d$  states. The resonance enhancement of the V  $3d$  state for the V  $2p$  core excitation and the high photoionization cross section of the Cu  $3d$  states compared with the O  $2p$  states are fully utilized in addition to the high resolutions in energy and momentum facilitated by recent instrument developments. Clear differences from the results of low photon energy ARPES have been observed for both materials by virtue of the high  $3d$  sensitivity as well as high bulk sensitivity. Coexistence of a quasiparticle peak with an incoherent peak is observed in the metallic phase of  $V_6O_{13}$ , whereas the quasiparticle peak collapses in the insulator phase, in which two incoherent peaks are observed. In  $SrCuO_2$ , the dispersive behavior of the spectra is well understood on the basis of the one-dimensional half-filled Hubbard model with  $U/t=7.5$  and  $U=3.0$  eV ( $U$ : Coulomb repulsive energy and  $t$ : transfer energy) and substantial coupling between the spin and charge excitations is suggested.

DOI: 10.1103/PhysRevB.70.155106

PACS number(s): 71.27.+a, 71.30.+h, 71.10.Pm, 71.20.-b

## I. INTRODUCTION

Angle-resolved photoemission spectroscopy (ARPES) with high resolutions in energy and momentum (or wave number  $k$ ) realized at low photon energies ( $h\nu$ ) between  $\sim 20$  and  $\sim 100$  eV has extensively been applied to correlated electron systems.<sup>1,2</sup> However, it is known that such a low  $h\nu$  photoemission spectroscopy (PES) is surface sensitive and often provides spectral shapes that are not consistent with bulk electronic structures in several transition metal and rare earth compounds.<sup>3-8</sup> For example, among accumulated low  $h\nu$  ARPES results for  $3d$  and  $4d$  transition metals and their compounds, some ARPES results are inconsistent with the results of such bulk sensitive measurements as the de Haas van Alphen studies because of the contribution of surface-characteristic electronic states. Therefore, caution is required in the photoemission spectroscopy to suppress surface effects sensitively probed by the short photoelectron mean free path ( $\lambda$ ) for the study of bulk electronic structures. Very often,  $\lambda$  has a minimum below 5 Å between 20 and 100 eV. To overcome this essential difficulty, the bulk sensitive ARPES

above several hundred eV with  $\lambda > 10$  Å has strongly been desired. High-energy ARPES is bulk sensitive but thought to be strongly influenced by the  $k$  averaging effects, on the other hand.

Pioneering ARPES with high  $h\nu$  was performed many years ago,<sup>9,10</sup> and the applicability of the direct-transition model and the rather weak dependence on the matrix element effects were reported. However, the unsatisfactory angular ( $\pm 2^\circ$ ) and energy (0.35–0.85 eV) resolutions made it impractical for band mapping and fermiology. The high  $h\nu$  and high resolution ARPES is very difficult because the photoionization cross section ( $\sigma$ ) decreases drastically with  $h\nu$  above 100 eV<sup>11</sup> and the energy resolution  $\Delta h\nu$  of the soft x ray is generally very poor.

Here we report an application of the soft x-ray ARPES by virtue of the high angular resolution and satisfactory energy resolution at several hundred eV enabled by instrument development. By the use of the state-of-the-art light source, a high quality monochromator, and a high performance electron analyzer, the high resolution soft x-ray ARPES became a reality<sup>12</sup> with the angular resolution of  $\pm 0.25^\circ$  and the total

energy resolution ( $\Delta E$ ) of  $\sim 100$  meV. The matrix element effects are much weaker in the soft x-ray ARPES at several hundred eV than for the low  $h\nu$  ARPES.

By this means, we have challenged the bulk-sensitive ARPES studies of two typical quasi-one-dimensional (1D) correlated electron systems:  $V_6O_{13}$  and  $SrCuO_2$ , which show the metal-to-insulator transition (MIT) and the so-called “spin-charge separation,” respectively, to be very important subjects in strongly correlated electron systems. We found for high kinetic energy ( $E_K$ ) photoelectrons excited near the Fermi level ( $E_F$ ): (1) direct transition effect is dominating far beyond the phonon induced  $k$  averaging, revealing the bulk intrinsic dispersions and (2) noticeable differences are present compared with the low  $h\nu$  ARPES.

## II. EXPERIMENTAL PROCEDURE

The soft x-ray PES and ARPES were performed at BL25SU of SPring-8 by using a circularly polarized light from a helical undulator, a high resolution varied line spacing plane grating monochromator and a SES200 electron analyzer. The surface normal of the sample was set parallel to the axis of the lens attached to a hemispherical analyzer, which was set to  $45^\circ$  from the light incidence direction. It is thought by considerable number of scientists as the non-negligible magnitude of the photon momentum  $q$  spoils the resolution in the wave number of ARPES. As demonstrated for a layered  $\eta$ - $Mo_4O_{11}$ ,<sup>13</sup> the wave number resolution in the soft x-ray ARPES is not deteriorated by the large photon momentum  $q$ , which is just transferred to the photoelectron momentum in the photoexcitation process. For  $h\nu=700$  eV, the photon momentum  $q$  is equal to  $0.36 \text{ \AA}^{-1}$ . The  $q_{\parallel}=0.25 \text{ \AA}^{-1}$  is then transferred to the photoelectron momentum parallel to the surface ( $k_{\parallel}$ ) according to the momentum conservation law. For a lattice constant of  $c=3.9 \text{ \AA}$  ( $SrCuO_2$ ), for example, the wave number at the Brillouin zone edge is  $\pi/c=0.80 \text{ \AA}^{-1}$ . Since  $k_{\parallel}$  is represented as  $0.51(E_K)^{1/2} \sin \theta \text{ (\AA}^{-1}\text{)}$ , where  $\theta$  is the emission angle from the surface normal, the instrumental angular resolution of  $0.25^\circ$  corresponds to the  $k_{\parallel}$  resolution of  $\sim 0.06 \text{ \AA}^{-1}$ , which is less than 10% of  $\pi/c$ . The total horizontal angular aperture of  $12^\circ$  (or  $\pm 6^\circ$  from the lens axis) separated into 127 segments corresponds to  $2.8 \text{ \AA}^{-1}$ , which is 1.76 times as large as  $2\pi/c$ . Thus, a mirror symmetry of the dispersion at the Brillouin zone center in the wide wave number region is really observed in our experiment, where only subtraction of the offset  $q_{\parallel}$  is required for the evaluation of  $k_{\parallel}$ . Such results have demonstrated the validity of our argument. The angular acceptance perpendicular to this direction is about  $\pm 0.25^\circ$  for ARPES. The angular acceptance for the angle integrated measurement is set to around  $\pm 3^\circ$  (The other acceptance angle perpendicular to this is  $12^\circ$ .)

High quality  $V_6O_{13}$  and  $SrCuO_2$  single crystals were *in situ* cleaved at about 130 and 300 K, providing the  $a$ - $b$  and  $a$ - $c$  specular surfaces, respectively. We performed the angle integrated PES and ARPES measurements at 180 and 100 K for  $V_6O_{13}$  and at 300 K for the insulating  $SrCuO_2$ , where no charging up effect was observed. The Fermi level was calibrated by a Au thin film.

## III. RESULTS AND DISCUSSION

### A. $V_6O_{13}$

$V_6O_{13}$  is a layered material with a quasi-1D behavior due to the V chains along the  $b$  axis.<sup>14–16</sup> This material is metallic (M) above  $T_I \sim 145$  K and insulating (I) below it (antiferromagnetic below  $T_N=55$  K). The valence mixing is taking place in the M phase with three inequivalent V sites of nominally  $V^{4+}(3d^1)$  and  $V^{5+}(3d^0)$  (with the ratio of 2 to 1). Three kinds of distorted  $VO_6$  octahedra run along the  $b$  axis by edge sharing. According to x-ray diffraction,<sup>15</sup> V(1) $O_6$  octahedra form single zigzag strings with the effective V valence of 4.16, whereas V(2) $O_6$  and V(3) $O_6$  octahedra form double zigzag strings with effective V valences of 4.60 and 4.34, respectively. Namely, it is suggested that V(1) and V(3) have a  $V^{4+}$ -like character and V(2) has a  $V^{5+}$ -like character in the M phase.<sup>16</sup> Below the first order MIT are reported the charge redistribution and the presence of the paramagnetic  $V^{4+}$  and singlet paired spin  $V^{4+}$ , as well as  $V^{5+}$  states. It is reported in the I phase at 120 K that the loss of the mirror plane symmetry induces the atoms to move vertically along the  $b$  axis with a coincident twinning. The resultant charge redistribution is reported to make the valences as  $\sim 4.4$  for V(1),  $\sim 4.4$  for V(2) and  $\sim 4.2$  for V(3) at 120 K.<sup>15</sup> Although these values may be not so accurate, it is thought as V(2) forms a  $V^{4+}$  spin singlet pair and V(3) corresponds to the paramagnetic  $V^{4+}$  and V(1) corresponds to  $V^{5+}$  site.<sup>15</sup> Through the MIT, the V(1) site becomes more  $V^{5+}$ -like, while both V(2) and V(3) sites become more  $V^{4+}$ -like.

We have performed the angle integrated PES measurements with the resolution of 80 meV at several  $h\nu$  and selected 515.7 eV, the low energy threshold of the main V  $2p$ - $3d$  absorption, to resonantly excite the V  $3d$  component and still do not induce noticeable Auger features. Under this condition, the V  $3d$  spectral weight is one order of magnitude larger than that of the O  $2p$  state.

We then performed ARPES along the  $b$  axis of  $V_6O_{13}$  with the energy resolution of 160 meV to realize an acceptable signal to noise ratio. The polar angle  $\theta$  for the ARPES in Fig. 1 covers the region from  $-6^\circ$  to  $+5^\circ$ . The raw energy distribution curves (EDC) of ARPES in both M and I phases are given in Fig. 1(a). No noticeable dispersion was seen perpendicular to the  $b$  axis. Figure 1(b) shows the angle integrated PES with the energy resolution of 80 meV, demonstrating a detailed change of the EDC on MIT. In the M phase at 180 K,  $E_F$  crosses the rising part of EDC beyond the instrument resolution and thermal broadening. In addition, a strong peak is observed at the binding energy  $E_B=0.70$ – $0.75$  eV. In the I phase at 100 K, however, a band-gap of  $\sim 120$  meV is observed by extrapolating the EDC threshold to zero intensity. This gap is noticeably smaller than the gap of  $\sim 0.2$  eV, as revealed by the low  $h\nu$  ARPES.<sup>17</sup> A strong peak is observed in 0.5–0.7 eV. In addition, a clear hump is reproducibly observed near 1.5 eV in our spectra, whereas such a feature is absent in the low- $h\nu$  PES<sup>14</sup> and ARPES.<sup>17</sup>

More details are obtained from ARPES. Figure 1(c) shows the density plot of the ARPES given in Fig. 1(a) and the corresponding momentum distribution curves (MDC) are

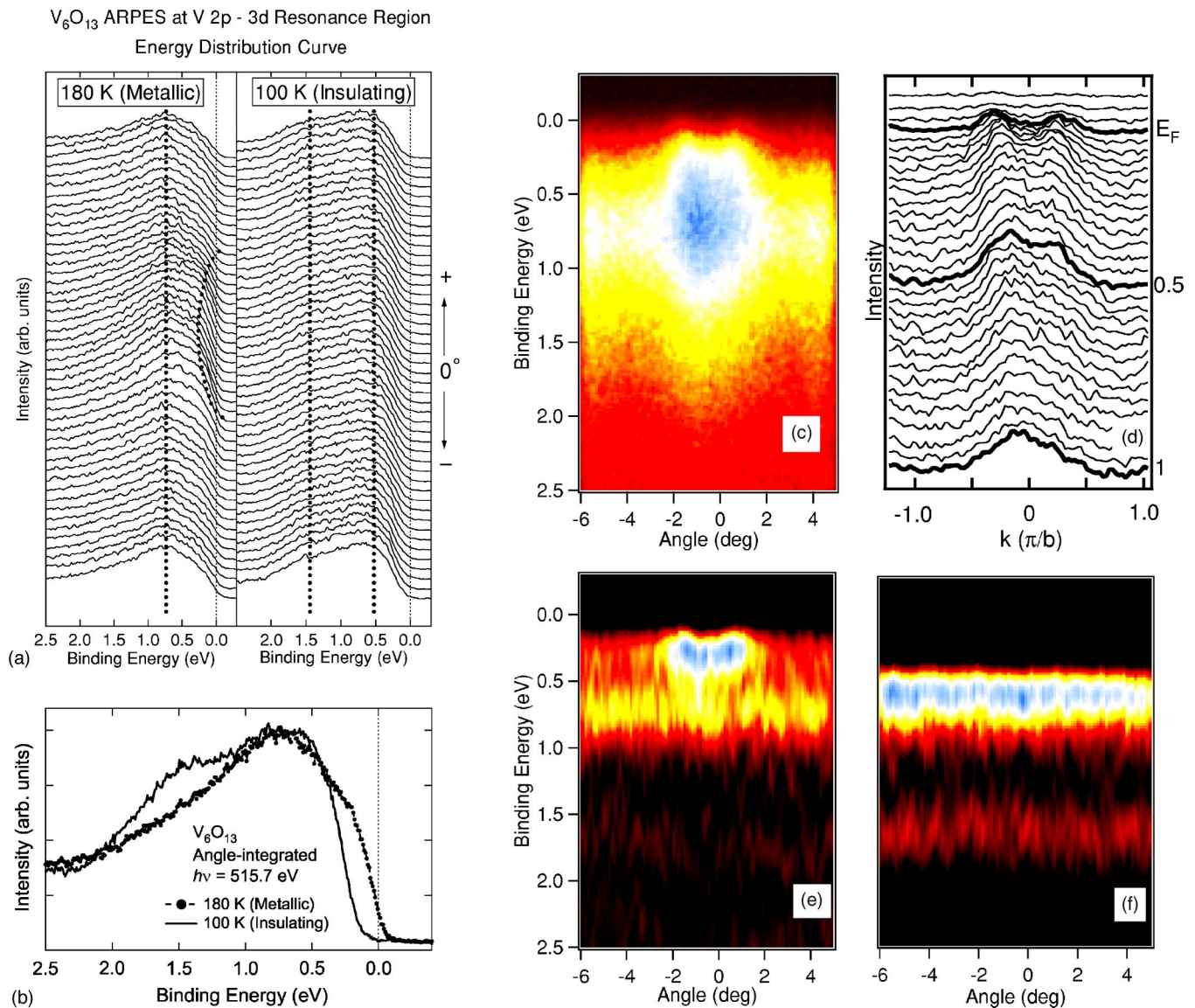


FIG. 1. ARPES and PES of  $V_6O_{13}$  at  $h\nu=515.7$  eV. (a) Raw ARPES EDC of  $V_6O_{13}$  in the metallic (M) and insulator (I) phases at 180 and 100 K with the energy resolution of 160 meV. The polar angle ranges from  $-6^\circ$  to  $5^\circ$ . Hereafter, the  $\theta$  values are given after correcting the photon  $q_{\parallel}$ . (b) Angle integrated PES at 180 and 100 K measured with the energy resolution of 80 meV. (c) Density plot of ARPES. (d) Momentum distribution curves (MDC). (e) Second energy derivative for the M phase at 180 K. (f) Second energy derivative for the I phase at 100 K.

shown in Fig. 1(d), where a branch crossing  $E_F$  with noticeable intensity on both sides of  $\theta=0^\circ$  near  $k_{\parallel}=0.30\pi/b$  is directly seen. This structure corresponds to a quasiparticle or a coherent peak. Although the decrease of the PES intensity toward  $E_F$  is often observed for quasi-1D systems, the result in Fig. 1(d) together with the finite EDC intensity at  $E_F$  in Fig. 1(b) are different from what is predicted for a Tomonaga-Luttinger-liquid<sup>18</sup> for 1D system, and therefore suggests the non-negligible three-dimensional (3D) character of the relevant electronic states in the M phase of  $V_6O_{13}$ .

In the MDC it is found that the dispersion below  $E_F$  is larger than 0.5 eV, with its bottom located at the  $\Gamma$  point ( $k_{\parallel}=0$ ). Thus, the soft x-ray ARPES under the resonance excitation enabled the resolution of  $k$  and band mapping. The second energy derivatives of the results in Fig. 1(a) are dis-

played in Figs. 1(e) and 1(f). The dispersive quasiparticle peak in the M phase is coexisting in the same  $k$  region with the incoherent peak at 0.7–0.75 eV, which is ascribed to the lower Hubbard band (LHB). Thus, the electron correlation energy or the on-site Coulomb repulsive energy  $U$  is estimated as  $\sim 1.4$ – $1.5$  eV. If the transfer energy  $t$  is taken as  $\sim 0.5$  eV,  $U/t$  is estimated to be  $\sim 2.8$ – $3$  for the M phase of  $V_6O_{13}$ . The quasiparticle peak crossing  $E_F$  is ascribed to the electronic state in the plane with the  $V^{4+}$  and  $V^{5+}$  valence mixing, whereas the prominent incoherent state in Fig. 1(e) is ascribed to that in the plane with the different V valence.<sup>15,16</sup> More specifically, the valence mixing between V(3) and V(2) is responsible for the coherent part and V(1) is responsible for the incoherent peak in the M phase. The Curie-Weiss paramagnetism due to the local magnetic mo-

ment in the M phase results from the V(1) site. In the M phase of the  $d^2$  system  $V_2O_3$  ( $d^1$  system  $SrVO_3$ ), a strong incoherent peak is located near 1.2 eV (1.6 eV) in addition to the coherent peak crossing  $E_F$ .<sup>19,20</sup> Analogously, the incoherent part corresponding to the quasiparticle is hidden in the high  $E_B$  tail of the EDC in Figs. 1(a) and 1(b).

In the I phase, however, the quasiparticle peak near  $E_F$  is collapsed. Instead, an incoherent peak is observed near 1.5 eV in addition to an incoherent structure at 0.5–0.7 eV in Fig. 1(f). These two incoherent structures observed in the bulk-sensitive as well as V 3d-sensitive measurement near 0.5–0.7 and 1.5 eV in the I phase are interpreted as resulting from the LHB due to the crystallographically inequivalent  $V^{4+}$  sites<sup>15,16</sup> with essentially different valences. It is seen that the incoherent peak in the M phase is shifted slightly toward smaller  $E_B$  in the I phase. Since V(1) site is thought to be responsible for this peak, the increase of the valence from 4.16 in the M phase to 4.4 in the I phase may be responsible for such a change because of the reduction of the  $d$  electron number. On the other hand, the reduction of the valence of the V(3) and V(2) sites in the I phase results in the increase of the  $d$  electron number, providing a very prominent incoherent peak near 1.5 eV.

These energies of the incoherent peaks are much different from those reported at 21.2 eV near 0.8–1.0 and 0.4–0.5 eV in the I phase.<sup>17</sup> This remarkable difference between high and low  $h\nu$  ARPES is due to the V 3d sensitivity in our V 2p-3d resonant photoemission experiment in comparison with the O 2p sensitivity in the low  $h\nu$  experiment (in which the V 3d cross section is a few times smaller than that of the O 2p state<sup>11</sup>) as well as to the bulk sensitivity<sup>19,20</sup> of our experiment. The energy difference of the V 3d coherent peak on the surface and in the bulk is already seen in the case of  $V_2O_3$ .<sup>19</sup> Even when one probes the O 2p state well hybridized with the V 3d state, its peak energy on the surface will be deviated from that in the bulk because of such an origin. Surface degradation is observed after several hours even in our rather bulk-sensitive ARPES. When  $\lambda$  is in the range of 3–5 Å in the low- $h\nu$  ARPES, the results are much more sensitive to the surface degradation.

The M phase of  $V_6O_{13}$  can be regarded as a quasi-1D metallic system. Although two V 3d branches, namely, a simply dispersive quasiparticle and incoherent peak(s), are observed, they are ascribed to different V sites. Clear separation of the dispersive peak into the spinon and holon branches is not seen in our measurement in contrast to the spin-charge separation scenario.<sup>21,22</sup> This may be due to the aforementioned non-negligible 3D character<sup>15,16</sup> as well as to the coupling between the spin and charge excitations due to the small  $U/t \sim 3$  in the M phase of  $V_6O_{13}$ , as discussed later in more detail for  $SrCuO_2$ .

### B. $SrCuO_2$

In the 1D antiferromagnetic insulator  $SrCuO_2$ , the double Cu-O chains are lined parallel to the  $c$  axis.<sup>23,24</sup> The inter-chain coupling is much weaker than the intrachain interaction. The cleavage is done between two Sr-O planes. Thus, the Cu-O chains correspond to the second and third planes as

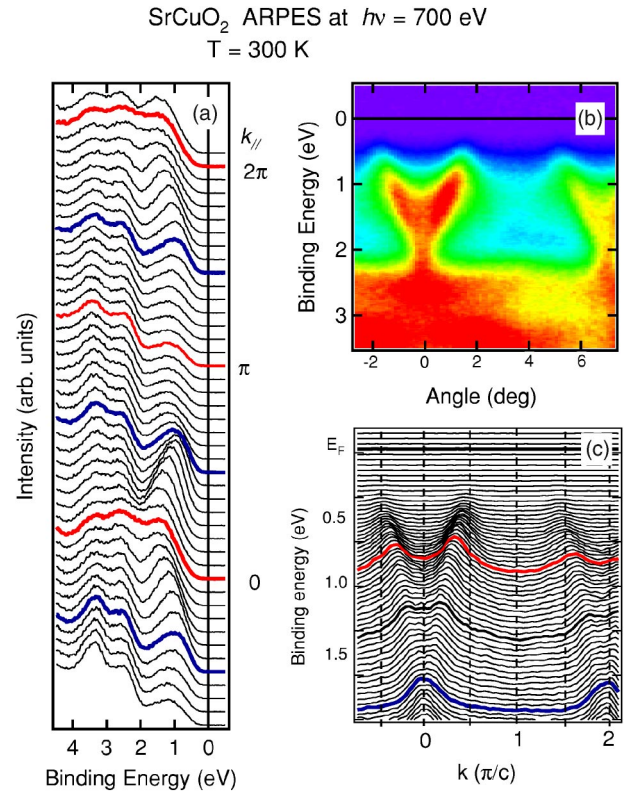


FIG. 2. Soft x-ray ( $h\nu=700$  eV) ARPES along the  $c$  axis of 1D  $SrCuO_2$  at 300 K. (a) EDC. (b) Density plot of the measured photoemission intensity. (c) MDC.

well as to the sixth and seventh planes from the surface, which could be probed within the photoelectron mean free path  $\lambda$  for the kinetic energy near 700 eV.<sup>25</sup> The ARPES measured along the  $k_{\parallel}$  parallel to the chain axis at  $h\nu = 700$  eV is summarized in Fig. 2(a). The photoionization cross section  $\sigma$  for the Cu 3d state is one order of magnitude larger than that for the O 2p state at this  $h\nu$ . These EDC shows that there is a clear bandgap between the top of the observed bands and  $E_F$ . The double peak structures in the region of 2–4 eV are ascribed to the so called “O 2p bands” in which the Cu 3d components are strongly hybridized. Meanwhile, the structure within 2 eV from  $E_F$  shows a prominent dispersion, as seen in the intensity density plot in Fig. 2(b). The shallowest peak is seen in Fig. 2(a) around 0.95 eV near the angle corresponding to  $(\pi/2, 0)$ . The peak shift from  $(0, 0)$  to  $(\pi/2, 0)$  is 0.5–0.6 eV. The MDC is shown in Fig. 2(c). The dispersion in the MDC is rather V shaped with a bottom at the  $\Gamma$   $(0, 0)$  point at around 1.9 eV, and the gap is estimated to be less than 0.5 eV from  $E_F$ . The  $k$  averaging effect by phonon scattering<sup>9,10</sup> is found to be not essential in  $SrCuO_2$  even for  $h\nu=700$  eV at 300 K, judging from the half-width of the EDC spectra and from the clear MDC peaks. To the direction perpendicular to the  $c$  axis, no dispersion was observed in the corresponding  $E_B$  region.

Here the present results are briefly compared with the results measured at  $h\nu=22.4$  eV.<sup>24,26</sup> Although the structures at  $h\nu=22.4$  eV with  $E_B < 1.5$  eV are much weaker than those of the O 2p bands, they are of comparable intensity at  $h\nu = 700$  eV, demonstrating the Cu 3d sensitivity of the ARPES

at  $h\nu=700$  eV. In the ARPES at  $h\nu=22.4$  eV, a steplike structure is observed near  $k_{\parallel}(\pi/c)=1.0$ <sup>24,26</sup> for  $k_{\perp}=1.0$  and  $0.4$ .<sup>27</sup> After subtracting this steplike structure, a single dispersion is deduced in the region of  $k_{\parallel}(\pi/2,0)-(\pi,0)$ . Reference 26 describes this steplike structure as due to scattered electrons and as having an empirical anticorrelation with the sample surface quality.<sup>28</sup> It is also stated that this signal is approximately isotropic and is thought to be handled as a background. One should notice, however, there are two branches in the  $(\pi/2,0)-(\pi,0)$  region in the low  $h\nu$  ARPES<sup>26</sup> if the steplike structure were not such a background, but an intrinsic structure. The structure we observe in the  $(\pi/2,0)-(\pi,0)-(3\pi/2,0)$  region corresponds to the smaller  $E_B$  component of these two structures. Considering the larger  $\lambda$  of the present ARPES, this structure cannot be a simple surface derived background. The present results never show the branch as in Fig. 2 of Ref. 24 and Figs. 3(d) and 5 in Ref. 26 with a dispersion up to 1 eV in the  $k_{\parallel}$  region of  $(\pi/2,0)-(\pi,0)$ .

Recall that the present high-energy ARPES results obtained by a circularly polarized light contain both components excited by the parallel and perpendicular polarizations to the  $c$  axis. In the ARPES at  $h\nu=22.4$  eV, the shallow branch in  $(0,0)-(\pi/2,0)$  ascribed to the spinon is observed only for the polarization parallel to the chain and for  $k_{\perp}=1.0$ , as shown in Fig. 5 of Ref. 26, and the dispersion for  $k_{\perp}=0.0$  is as large as 1.0 eV in the EDC spectra for the perpendicular polarization. Although our experiment includes both parallel and perpendicular polarizations, we do not see such a dispersion up to 1.0 eV in EDC, since the peak shift in EDC of our result is 0.5–0.6 eV. Thus, our rather bulk-sensitive results are much different from the low  $h\nu$  ARPES.

In the present results, the shallowest peak in the region of  $(\pi/2,0)-(\pi,0)-(3\pi/2,0)$  is significantly weaker than that in the  $(-\pi/2,0)-(0,0)-(\pi/2,0)$  region. The dispersion in the  $(\pi/2,0)-(\pi,0)-(3\pi/2,0)$  region is not larger than the dispersion in the  $(-\pi/2,0)-(0,0)-(\pi/2,0)$  region. In the MDC, any dispersive feature is not noticed in the  $(\pi/2,0)-(\pi,0)-(3\pi/2,0)$  region. Besides, no trace of any additional component is detected in the EDC and MDC in the  $(-\pi/2,0)-(0,0)-(\pi/2,0)$  region of ARPES in spite of the sufficient resolutions in energy and  $k_{\parallel}$  as well as the high Cu 3d sensitivity in the present experiment, providing no support to the multiple bands.<sup>26</sup>

In order to interpret the present ARPES of SrCuO<sub>2</sub>, we have employed the one-band, 1D half-filled Hubbard model<sup>29</sup> based on the quantum Monte Carlo calculation, in which the quantum fluctuation effects on the response function are completely included. The parameters to be employed are the transfer energy  $t$  (to the nearest-neighbor site) and the on-site Coulomb repulsive energy  $U$ . Parameters are selected to reproduce the behavior of the EDC (width, energy positions, and dispersion) as a function of  $k_{\perp}$  as well as of the MDC. A calculated result at 400 K for  $U/t=7.5$  ( $U=3.0$  eV and  $t=0.4$  eV) is shown in Fig. 3, which provides the peak shift of 0.5 eV and the shallowest peak at 0.95 eV. The MDC is given in the lower panel, where the V shaped dispersion is clearly reproduced and no dispersion is seen in

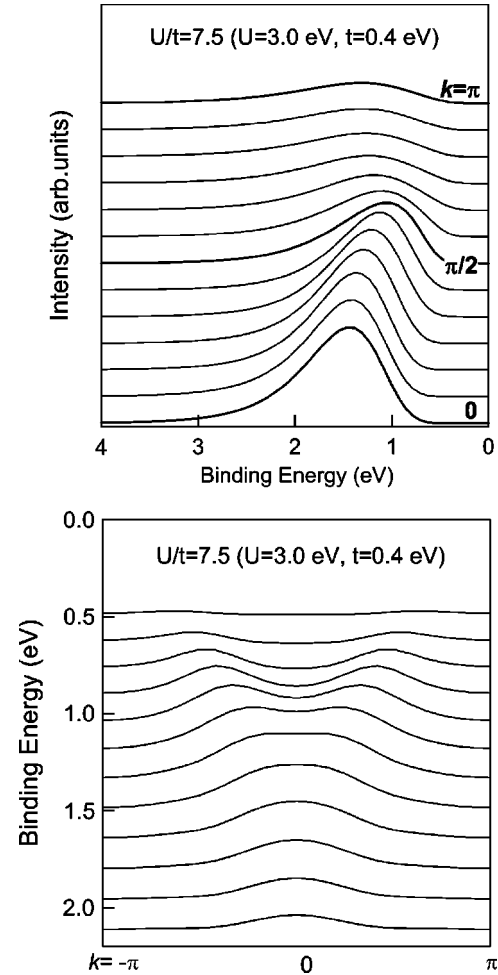


FIG. 3. ARPES calculated by one-band 1D half-filled Hubbard model at 400 K.  $U/t=7.5$  ( $U=3.0$  and  $t=0.4$  eV). EDC (upper) and MDC (lower).

the  $(\pi/2,0)-(\pi,0)$  region. In this model, the broad width of the main EDC peak corresponds to multimagnon excitations coupled with the photocreated hole.<sup>29</sup> In the infinite  $U$  case, as is well known, the spin and charge excitations are exactly decoupled. However, the present result shows that we still have significant spin-charge coupling in such a highly correlated electron system with  $U/t=7.5$  in the one-band 1D half-filled Hubbard model. In the MDC, it is recognized that the structure between  $E_B=0.9$  and  $0.6$  eV is not corresponding to the peak but to the tail of the ARPES EDC (upper panel). Since the PES at  $h\nu=700$  eV is almost ten times more sensitive to the Cu 3d states than to the O 2p states,<sup>11</sup> the results are ascribed mostly to the Cu 3d components, which are strongly renormalized by  $U$ ,  $t$ , and the magnon excitations. According to this model, the weaker structures observed in  $(\pi/2,0)-(\pi,0)$  corresponds to the incoherent component induced by the effect of electron correlation  $U$ .

The low energy ARPES<sup>24,26,27</sup> was interpreted by the  $t$ - $J$  model ( $J$  stands for the spin exchange interaction), in which the double occupancy of the same site is excluded by considering the large  $U$ . As a result, the dispersions from  $(0,0)$  to  $(\pi/2,0)$  were ascribed to both spinon and holon as well as to their mixed excitations, whereas only the holon dispersion

was predicted in the  $(\pi/2, 0) - (\pi, 0)$  region. The values of  $t \sim 0.6$  and  $J \sim 0.2$  eV were employed there for SrCuO<sub>2</sub> ( $U$ , approximated by  $4t^2/J$ , becomes as large as 7.2 eV, resulting in  $U/t \sim 12$ ). However, this picture seems too simplified to explain the present bulk-sensitive ARPES, in which the observed dispersion is much different from that observed by the low  $h\nu$  ARPES, and the spinon and holon branches are not separated despite sufficient energy and momentum resolutions. We suggest that the coupling between the spin and charge might play an important role in the present bulk-sensitive ARPES for SrCuO<sub>2</sub>.

By explicitly taking both Cu  $3d$  and O  $2p$  states and their mutual hybridization, the  $p$ - $d$  model was also applied to SrCuO<sub>2</sub>,<sup>26</sup> predicting that the Cu  $3d$  (O  $2p$ ) component is predominant near  $k=(0, 0)$  [ $k=(\pi, 0)$ ], whereas they are comparable near  $(\pi/2, 0)$ . The non-negligible intensity near  $(\pi, 0)$  in the present Cu  $3d$  sensitive result cannot be explained by this model calculation with the parameters employed in Fig. 7 of Ref. 26. Even though our experiment is very sensitive to the Cu  $3d$  states, separation of the structures into spinon and holon branches is not observed in the  $(-\pi/2, 0) - (0, 0) - (\pi/2, 0)$  region, which suggests an appreciable coupling between these excitations. Moreover, the peak shift of the shallowest peak in the EDC up to 0.5–0.6 eV and the dispersion in the MDC in the  $(0, 0) - (\pi/2, 0)$  region up to 1.4 eV are smaller or comparable to the result of linear augmented plane wave calculation<sup>30</sup> and not much larger than the latter, suggesting that the spin-charge separation is not prerequisite to understand the ARPES results from this comparison.

In this way, the  $p$ - $d$  and  $t$ - $J$  model analyses of the available low  $h\nu$  ARPES are not consistent with the results of our high-energy ARPES. Our experimental results are noticeably different from the low  $h\nu$  ARPES but are well understood by the one-band, 1D half-filled Hubbard model with  $U/t=7.5$  and  $U=3.0$  eV as mentioned before. It is possible that the low  $h\nu$  ARPES most sensitively probes the O  $2p$  components of the chain closest to the cleaved surface, which is liable to

be influenced by the surface conditions,<sup>26,28</sup> whereas our experiments at  $h\nu=700$  eV are probing the Cu  $3d$  components of four Cu-O chains from the surface, which are less influenced by such conditions.

#### IV. CONCLUSION

In summary, we have demonstrated for a quasi-1D metal and an insulator of transition-metal oxides that the high-energy ARPES in the several-hundred eV region is feasible to probe the dispersions and details of strongly correlated electronic structures through the relatively large photoionization cross section  $\sigma$  of the late transition metal  $3d$  states or their resonance enhancement for  $2p$  core excitation in early transition metal compounds. The ARPES at  $h\nu=515.7$  eV and  $h\nu=700$  eV is found to be noticeably different from those at  $h\nu=21.2$  and 22.4 eV for V<sub>6</sub>O<sub>13</sub> and SrCuO<sub>2</sub>, respectively. The differences are not only ascribable to the V  $3d$  and Cu  $3d$  sensitivity compared with the O  $2p$  sensitivity, but also to the larger photoelectron mean free path  $\lambda$  at higher photoelectron kinetic energies (10–15 Å compared with 3–5 Å by 20–100 eV ARPES). The non-negligible coupling between the spin and charge excitations is suggested from the present high-energy ARPES for both V<sub>6</sub>O<sub>13</sub> and SrCuO<sub>2</sub> without an extremely large  $U/t$ .

*Note added in proof.* Low energy ARPES of extra-charge-doped Sr<sub>2</sub>CuO<sub>3+ $\delta$</sub>  with single Cu-O chain measured at 15.2 eV is reported in Ref. 31. Two structures are seen near the (0,0) point. It is reported that the shallowest branch is not resolved in the undoped system.

#### ACKNOWLEDGMENT

This work was partially supported by a Grant-in-Aid for Creative Scientific Research (15GS0213) of Mext, Japan and JASRI (Proposal 2001B1009-LS-np). The authors acknowledge J. Igarashi, Z.-X. Shen, C. Kim, T. Tohyama, and S. Maekawa for fruitful discussions.

<sup>1</sup>D. E. Eastman, F. J. Himpsel, and J. A. Knapp, Phys. Rev. Lett. **40**, 1514 (1978).

<sup>2</sup>Y. Petroff and P. Thiry, Appl. Opt. **19**, 3957 (1980).

<sup>3</sup>A. Damascelli, Z. X. Shen, and Z. Hussain, Rev. Mod. Phys. **75**, 473 (2003).

<sup>4</sup>D. Lynch and C. G. Olson, *Photoemission Studies of High-Temperature Superconductors* (Cambridge University Press, Cambridge, 1999).

<sup>5</sup>A. P. Mackenzie, S. R. Julian, G. G. Lonzarich, Y. Maeno, and T. Fujita, Phys. Rev. Lett. **78**, 2271 (1997).

<sup>6</sup>J. W. Allen, *Resonant Photoemission of Solids with Strongly Correlated electrons*, Synchrotron Radiation Research: Advances in Surface and Interface Science Vol. 1: techniques (Plenum, New York, 1992).

<sup>7</sup>K. Breuer, S. Messerli, D. Purdie, M. Garnier, M. Hengsberger, and Y. Baer, Phys. Rev. B **56**, R7061 (1997).

<sup>8</sup>A. Sekiyama, T. Iwasaki, K. Matsuda, Y. Saitoh, Y. Onuki, and S.

Suga, Nature (London) **403**, 396 (2000).

<sup>9</sup>Z. Hussain, E. Umbach, J. J. Barton, J. G. Tobin, and D. A. Shirley, Phys. Rev. B **25**, 672 (1982).

<sup>10</sup>R. C. White, C. S. Fadley, M. Sagurton, and Z. Hussain, Phys. Rev. B **34**, 5226 (1986).

<sup>11</sup>J. J. Yeh and I. Lindau, At. Data Nucl. Data Tables **32**, 1 (1985).

<sup>12</sup>S. Suga and A. Sekiyama, J. Electron Spectrosc. Relat. Phenom. **114–116**, 659 (2001).

<sup>13</sup>S. Suga, Surf. Rev. Lett. **9**, 1221 (2002).

<sup>14</sup>S. Shin, S. Suga, M. Taniguchi, M. Fujisawa, H. Kanzaki, A. Fujimori, H. Daimon, Y. Ueda, K. Kosuge, and S. Kachi, Phys. Rev. B **41**, 4993 (1990).

<sup>15</sup>P. D. Dernier, Mater. Res. Bull. **9**, 955 (1974).

<sup>16</sup>M. Itoh, H. Yasuoka, Y. Ueda, and K. Kosuge, J. Phys. Soc. Jpn. **53**, 1847 (1984).

<sup>17</sup>R. Eguchi, T. Yokoya, T. Kiss, Y. Ueda, and S. Shin, Phys. Rev. B **65**, 205124 (2002).

- <sup>18</sup>H. Ishii *et al.*, Nature (London) **426**, 540 (2003).
- <sup>19</sup>S.-K. Mo *et al.*, Phys. Rev. Lett. **90**, 186403 (2003).
- <sup>20</sup>A. Sekiyama, Phys. Rev. Lett. (in press).
- <sup>21</sup>H. Suzuura and N. Nagaosa, Phys. Rev. B **56**, 3548 (1997).
- <sup>22</sup>R. Claessen, M. Sing, U. Schwingenschlogel, M. Dressel, and C. S. Jacobsen, Phys. Rev. Lett. **88**, 096402 (2002); M. Sing, U. Schwingenschlogel, R. Claessen, P. Blaha, J. M. P. Carmelo, L. M. Martelo, P. D. Sacramento, M. Dressel, and C. S. Jacobsen, Phys. Rev. B **68**, 125111 (2003).
- <sup>23</sup>N. Motoyama, H. Eisaki, and S. Uchida, Phys. Rev. Lett. **76**, 3212 (1996).
- <sup>24</sup>C. Kim, A. Y. Matsuura, Z.-X. Shen, N. Motoyama, H. Eisaki, S. Uchida, T. Tohyama, and S. Maekawa, Phys. Rev. Lett. **77**, 4054 (1996).
- <sup>25</sup>S. Tanuma, C. Powell, and D. R. Penn, Surf. Sci. **192**, L849 (1987).
- <sup>26</sup>C. Kim, Z.-X. Shen, N. Motoyama, H. Eisaki, S. Uchida, T. Tohyama, and S. Maekawa, Phys. Rev. B **56**, 15589 (1997).
- <sup>27</sup>C. Kim, J. Electron Spectrosc. Relat. Phenom. **117–118**, 503 (2001).
- <sup>28</sup>H. Fujisawa, T. Yokoya, T. Takahashi, M. Tanaka, M. Hasegawa, and H. Takei, J. Electron Spectrosc. Relat. Phenom. **88–91**, 461 (1998).
- <sup>29</sup>N. Tomita and K. Nasu, Phys. Rev. B **60**, 8602 (1999). The peak position and the magnitude of dispersion are sensitive to  $U$  and  $t$ , respectively.
- <sup>30</sup>N. Nagasako, T. Oguchi, H. Fujisawa, O. Akaki, T. Yokoya, T. Takahashi, M. Tanaka, M. Hasegawa, and H. Takei, J. Phys. Soc. Jpn. **66**, 1756 (1997). Although the calculation provided a metallic feature, SrCuO<sub>2</sub> is a Mott insulator due to the electron correlation effect.
- <sup>31</sup>T. Valla, T. E. Kidd, P. D. Johnson, K. W. Kim, C. C. Homes, and G. D. Gu, cond-mat/0403486.